1-1-2016

Characterization of designed cobaltacarborane porphyrins using conductive probe atomic force microscopy

Venetia D. Lyles
Louisiana State University

Wilson K. Serem
Louisiana State University

Erhong Hao
Louisiana State University

M. Graça H. Vicente
Louisiana State University

Jayne C. Garno
Louisiana State University

Recommended Citation

Lyles, V., Serem, W., Hao, E., Vicente, M., & Garno, J. (2016). Characterization of designed cobaltacarborane porphyrins using conductive probe atomic force microscopy. *AIMS Materials Science, 3* (2), 380-389. https://doi.org/10.3934/matersci.2016.2.380

AIMS Materials Science, 3(2): 380-389.
DOI: 10.3934/matersci.2016.2.380
Received: 01 March 2016
Accepted: 16 March 2016
Published: 21 March 2016

http://www.aimspress.com/journal/Materials

Research article

Characterization of designed cobaltacarborane porphyrins using conductive probe atomic force microscopy

Venetia D. Lyles, Wilson K. Serem, Erhong Hao, M. Graça H. Vicente, and Jayne C. Garno*

Louisiana State University, Department of Chemistry, Baton Rouge LA, 70803, USA

* **Correspondence:** E-mail: jgarno@lsu.edu.

Abstract: Porphyrins and metalloporphyrins have unique chemical and electronic properties and thus provide useful model structures for studies of nanoscale electronic properties. The rigid planar structures and π-conjugated backbones of porphyrins convey robust electrical characteristics. For our investigations, cobaltacarborane porphyrins were synthesized using a ring-opening zwitterionic reaction to produce isomers with selected arrangements of carborane clusters on each macrocycle. Experiments were designed to investigate how the molecular structure influences the self-organization, surface assembly, and conductive properties of three molecular structures with 2, 4, or 8 cobaltacarborane substituents. Current versus voltage (I-V) spectra for designed cobaltacarborane porphyrins deposited on conductive gold substrates were acquired using conductive probe atomic force microscopy (CP-AFM). Characterizations with CP-AFM provide capabilities for obtaining physical measurements and structural information with unprecedented sensitivity. We found that the morphology of cobaltacarborane porphyrin structures formed on surfaces depends on a complex interplay of factors such as the solvent used for dissolution, the nature of the substrate, and the design of the parent molecule. The conductive properties of cobaltacarborane porphyrins were observed to change according to the arrangement of cobaltacarborane substituents. Specifically, the number and placement of the cobaltacarborane ligands on the porphyrin macrocycle affect the interactions that drive porphyrin self-assembly and crystallization. Interestingly, coulombic staircase I-V profiles were detected for a porphyrin with two cobaltacarborane substituents.

Keywords: porphyrin; conductive probe AFM; cobaltacarborane porphyrin

1. Introduction

The choice of studying model systems of porphyrins is highly practical, because of the associated properties of this functional class of molecules. Porphyrin and metalloporphyrin systems are excellent materials for molecular electronics, due to their diverse structural motifs and associated electrical, optical and chemical properties, and thermal stability [1–6]. At a basic level, electronic properties are controlled by the degree of π delocalization [7]. Porphyrins can be organized into supramolecular arrays, aggregates and crystals with diverse functions. The rigid planar structures and π- conjugated backbone of porphyrins convey robust electrical characteristics. The porphyrin macrocycle consists of four pyrrole rings joined by four methine carbons. The architecture of porphyrins has been proposed as viable for electronic components for molecular-based information-storage devices [8–11], gas sensors [12,13], photovoltaic cells [14,15], organic light-emitting diodes [16–19], and molecular wires [20,21,22].

Synthesis of cobaltacarborane porphyrin conjugates was first reported by Vicente et al [23,24,25]. The cobaltacarborane ligand consists of an alkoxy chain terminated with two carborane cages with a single cobalt atom situated between the carboranes [23–27]. The abundance of boron in the cobaltacarborane ligands was studied for potential applications in boron neutron capture therapy [23,24]. The cobaltabisdicarbollide anion in the cobaltacarborane ligand were studied for attributes of chemical, thermal, and photostability [5,24]. In this report, the conductive properties of selected cobaltacarboranes were investigated for potential applications in molecular electronics.

Research in the molecular electronics field has been advanced by the invention of the scanning tunneling and atomic force microscopes. Scanning probe microscopes have advantages for investigating nanoscale phenomena, with capabilities to acquire images with nanometer resolution as well as to make spectroscopy measurements of single molecules or clusters [28]. Scanning probe techniques (e.g. scanning tunneling microscopy, conductive probe AFM, scanning ionic capacitance microscopy, scanning electrochemical microscopy, Kelvin Probe AFM, electrostatic force AFM) can be used to obtain electronic information of molecular systems [28–33]. Scanning probe measurements have been used to examine electronic properties such as conductance, dielectric constants and capacitance while providing surface views and topographic information of the samples [29–36]. For conductive probe atomic force microscopy (CP-AFM), a conductive tip is scanned across the sample, while a bias is applied to the substrate. Most commonly, the current is measured by a sensitive preamp, located near the probe. With CP-AFM, two types of data acquisition are possible: a conductive map of the sample surface and a current voltage profile of selected local areas of the surface. The feedback mechanism of CP-AFM is based on applying a chosen force set-point; therefore, the conductive AFM probe remains in direct contact with the sample during spectroscopy measurements.

For these investigations, selected cobaltacarborane porphyrins were investigated using contact mode and CP-AFM to evaluate the role of molecular structure for surface assembly, self-aggregation and conductive properties. Specifically, changes with surface measurements were evaluated and compared according to the numbers and arrangement of substituents.

2. Materials and Methods

2.1. Sample Preparation

Gold substrates, Au(111)/mica, were purchased from Agilent Technologies, Inc. (Chandler, AZ). Cobaltacarborane porphyrins were synthesized as previously reported [24]. The gold substrates were rinsed with deionized water, then a 15 μl drop of porphyrin solution (10^{-6} M) was deposited on the gold substrate and dried in ambient conditions overnight.

2.2. Atomic Force Microscopy (AFM)

Conductive probe atomic force microscopy (CP-AFM) experiments were accomplished in air with a model 5500 AFM/SPM from Agilent equipped with Picoscan v5.3 software. Triangular cantilevers with a tip radius of less than 35 nm, tip height of 20–25 μm and a force constant of 6.0 N m^{-1} were used for contact mode imaging and CP-AFM, the tips were acquired from MikroMasch (San Jose, CA). A copper wire was placed in physical contact with the gold substrate, so that a bias could be applied to the sample (± 10.0 V). Digital images were processed using Gwyddion software [37].

3. Results and Discussion

Tetraphenyl porphyrin macrocycles were functionalized with 2, 4, or 8 cobaltacarborane substituents arranged as shown in Figure 1. The cobaltacarborane porphyrins were synthesized via a ring-opening zwitterionic reaction in high yields (90–97%), as previously reported [23,38]. Each of the substituents contains a cobalt atom which is coordinated between two carborane cages. The numbers and arrangement of the cobaltacarboranes should systematically influence the measured I-V characteristics, thus providing a model surface material for CP-AFM.

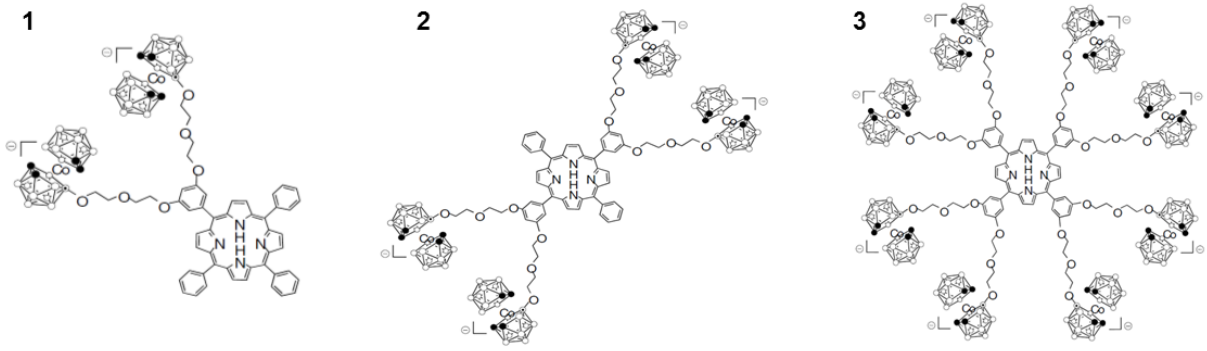

Figure 1. Cobaltacarborane porphyrins selected for AFM studies.

The symmetry of the molecules and arrangement of cobaltacarborane moieties was found to influence the surface assembly and molecular aggregation of samples prepared on Au(111). Representative images (topography and corresponding lateral force frames) of the three cobaltacarborane porphyrin (Co-Por) samples of Figure 1 are presented in Figure 2. Typically,

porphyrin macrocycles orient on the surface in a coplanar configuration, and stack together to form columnar assemblies. However, the nature and size of substituents influences the surface arrangement and self-aggregation of the nanocrystals. With two cobaltacarborane ligand for Co-Por **1**, the surface assemblies exhibit polydisperse sizes arranged randomly across the surface of gold (Figures 2A–2B). The nanocrystals tend to attach near the edges of the gold steps, however there is sufficient surface density for stacks to locate at terrace sites. The thickness and lateral dimensions of the nanostructures were disperse, however the geometry retained a nearly spherical shape. With four cobaltacarborane ligands oriented symmetrically as shown for Co-Por **2**, the surface structures changed to exhibit a rod-like or needle shape (Figures 2C–2D). There does not seem to be any preferential attachment to the edges of gold steps, the nanocrystals of Co-Por **2** are regularly shaped and randomly distributed throughout areas of the surface. With eight cobaltacarborane ligands, Co-Por **3** forms exquisitely regular spherical stacks that locate at the step edges of the gold surface (Figures 2E-2F). The vertical and lateral dimensions of the nanocrystals are relatively monodisperse, and tended to form linear assemblies that decorate step edges.

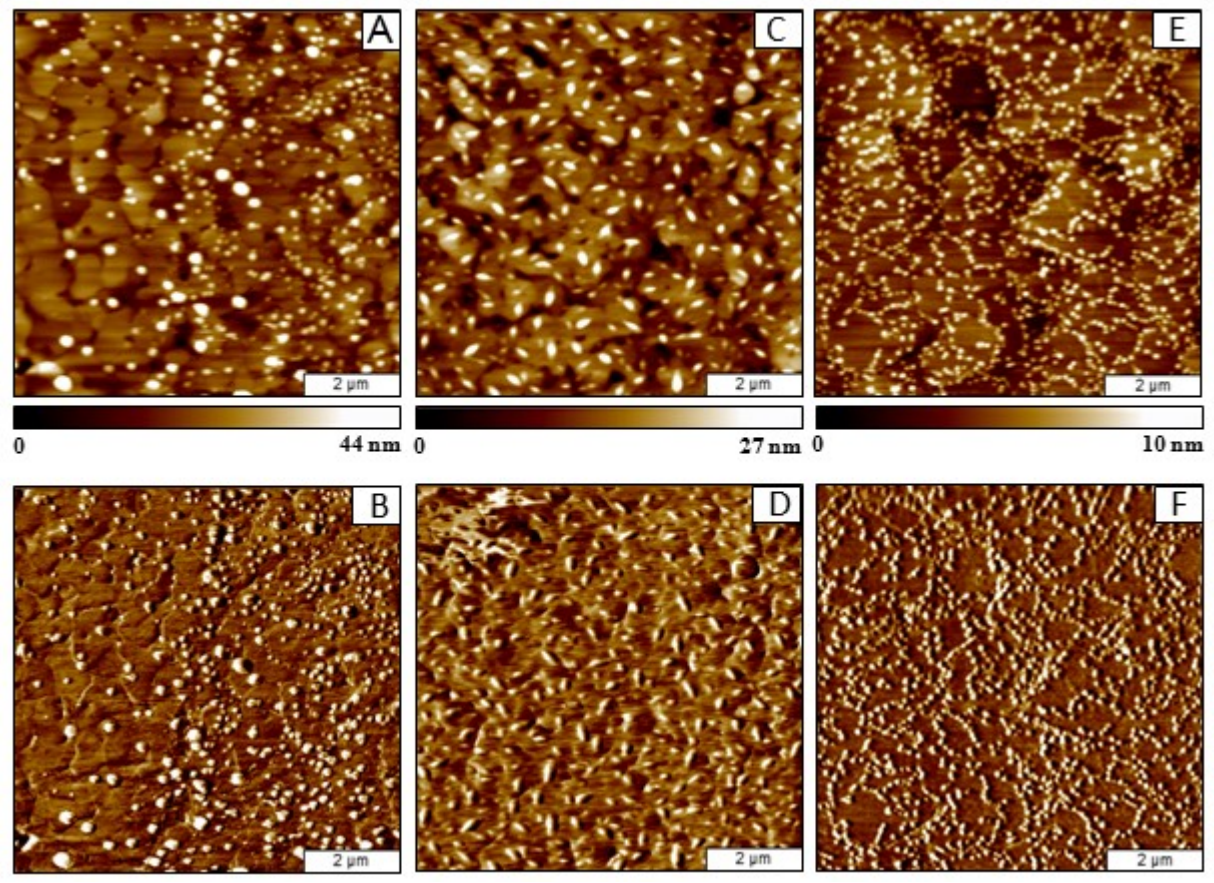

Figure 2. Cobaltacarborane porphyrin samples prepared on gold, imaged with contact mode AFM. The top row shows the topography frames, and the simultaneously acquired lateral force images are shown below. (A) Co-Por **1**, topography;(B) Co-Por **2**, lateral force frame; (C) Co-Por **2**, topography frame; (D) Co-Por **2**, lateral force frame; (E) Co-Por **3**, topography frame; (F) Co-Por **3**, lateral force image.

The systematic changes in surface shapes and dispersity highlight the role of molecular structure for surface assembly of the cobaltacarborane porphyrins. Previous studies with porphyrins have shown that pi-pi intermolecular interactions are a dominant force for directing macrocycles to assemble into stack structures, with the plane of the macrocycle aligning with the substrate. Differences in the number and placement of cobaltacarborane ligands led to changes in the shapes of surface assemblies, as well as in the arrangement to form linear chains or dispersed islands. The asymmetric arrangement of two cobaltacarborane ligands for Co-Por **1** produced a wider range of sizes and dispersity. The symmetric *para* arrangement of four ligands for Co-Por **2** produced elliptical rod shapes of symmetric crystals. A highly uniform spherical shape and size was observed for Co-Por **3**, with eight ligands arranged symmetrically around the macrocycle. The selected cobaltacarborane molecules nicely demonstrate that molecular symmetry directs the 3-D assembly of macromolecules to form nanocrystal shapes.

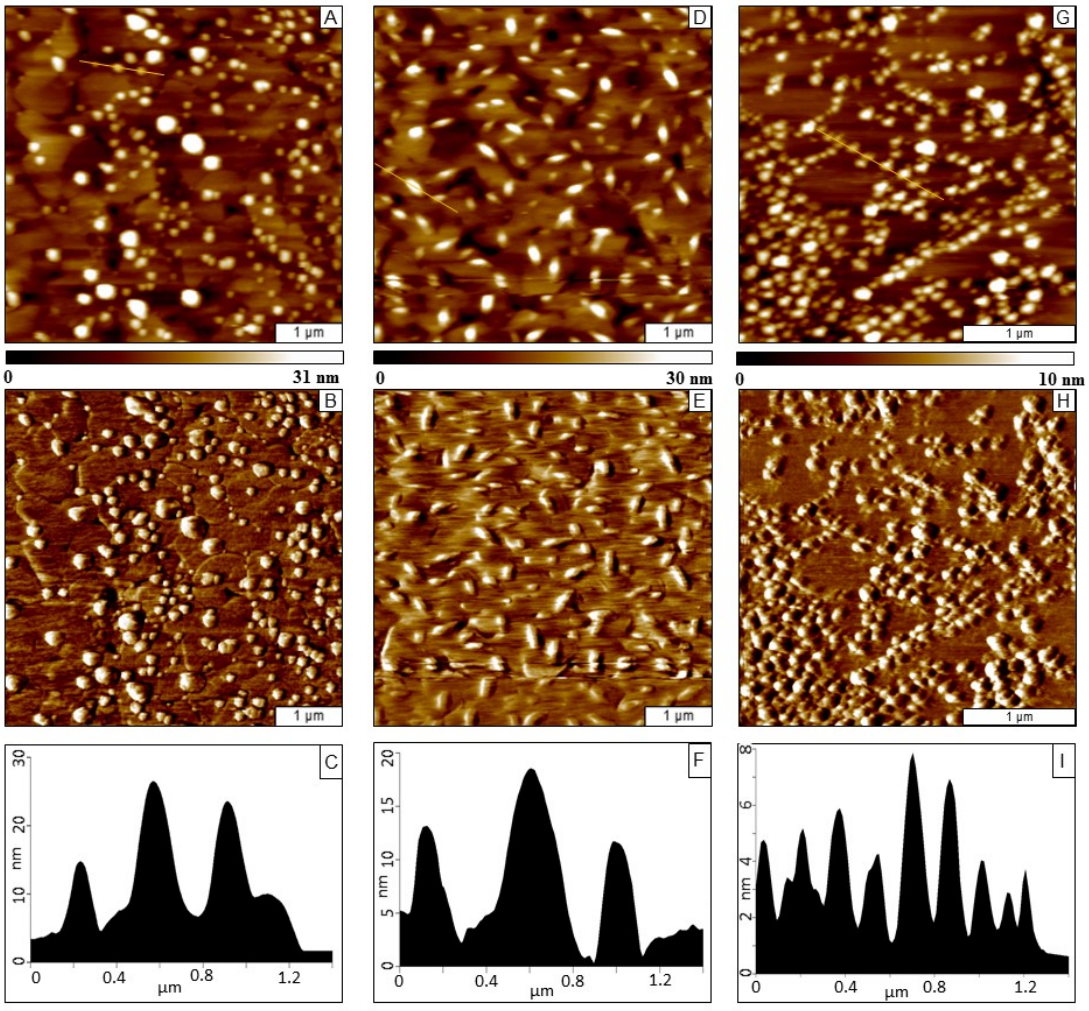

Figure 3. Magnified view of cobaltacarborane porphyrin nanocrystals on gold, imaged with contact mode AFM. (A) Topography; (B) lateral force and (C) example cursor profile for Co-Por **1**. (D) Topography; (E) lateral force and (F) corresponding cursor profile for Co-Por **2**.(G) Topography; (H) lateral force and (I) cursor profile for Co-Por **3**.

A zoom-in view of the cobaltacarborane porphyrin nanocrystals is shown side-by-side in Figure 3. The shapes and surface arrangement of each molecular structure are compared with topography frames in the top row, and the edges of the crystals are more clearly resolved in the corresponding lateral force images in the middle row. The heights of a few nanocrystals are shown with example cursor line profiles in the bottom panels. For the nonsymmetric structure of Co-Por **1** (Figures 3A and 3B) the nanocrystals have a mostly spherical shape, exhibiting a range of sizes. Many of the crystals are located at step edges, however a few are located within terrace sites. The step edges can be resolved in the lateral force frame, Figure 3B. A cursor profile indicated the heights of three nanocrystals of Co-Por **1** were 11, 23 and 18 nm, from left to right. In contrast, the rod-like shape of the para substituents of Co-Por **2** are viewed in Figures 3D and 3E. The segregated islands of Co-Por **2** do not appear to attach preferentially at sites of step edges and are randomly distributed across the surface. The heights of three nanocrystals outlined in Figure 3D were 11, 13, and 12 nm (Figure 3F).

A close-up view (3×3 μm^2) of densely packed nanostructures of Co-Por **3** is shown in Figures 3G-3H. At this magnification the linear arrangement of chains of near-spherical nanocrystals can be resolved, and some of the crystals have begun to pile together into taller aggregations. A cursor profile across nine nanocrystals (Figure 3I) indicates heights ranging from 2 to 8 nm.

The distribution of heights for the cobaltacarborane porphyrins is presented with size histograms in Figure 4. The widest range of sizes is observed for Co-Por **1**, ranging up to 40 nm in height with an average measuring 15 ± 7.2 nm. A smaller range of sizes (up to 25 nm in height) was observed for *tetra*-substituted Co-Por **2**, with an average height measuring 14 ± 3 nm. The narrowest size range and smallest nanostructures were observed for the *octa*-substituted Co-Por **3**, with an average height measuring 4 ± 1 nm. Porphyrin nanocrystals consist of multiple molecular layers assembled in a stacked arrangement. The cobaltacarborane ligands appear to interfere with the molecular self-assembly. The structure with the fewest ligands (Co-Por **1**) formed taller stacks, whereas increasing the numbers of substituents produced smaller structures. With a fully substituted arrangement with eight cobaltacarborane ligands, smaller crystals formed, likelydue to steric effects. Very slight changes in the concentration of the sample or the volume of deposited liquid can lead to polydispersity at the nanoscale. In the examples shown, the arrangement of cobaltacarborane substituents around the macrocycle also has an influence on the polydispersity and general size of the nanodots.

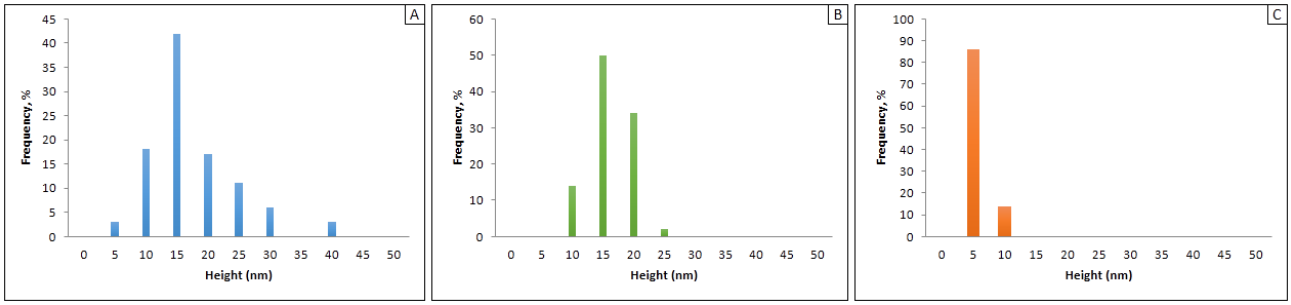

Figure 4. Height distribution measured with cursor profiles for cobaltacarborane porphyrins (n = 100): (A) Co-Por **1**; (B) Co-Por **2**; and (C) Co-Por **3**.

Representative current-voltage profiles of the cobaltacarborane porphyrins are compared in Figure 5. To ensure that the sample is not oxidized, a single measurement was made for each nanostructure, and the images shown are representative of multiple measurements within the sample area. The electrical transport properties of the three samples are distinct as regards the magnitude of the measured current and onset of conduction. A staircase profile was reproducibly detected for Co-Por **1**, indicative of Coulombic charging (Figure 5A). Discrete increments of 2 nA currentwere measured at approximately 1 V intervals for the molecule designed with two cobaltacarborane substituents. Coulombic behavior was not detected for the other samples. An I-V curve that is typical of a semiconductive sample was revealed for Co-Por **2**, with an asymmetric profile (Figure 5B). The onset of current was detected at −8 V and + 5 V, within a measuring range below 0.1 nA. The I-V profile for Co-Por **3** was also asymmetric, (Figure 5C) however the magnitude of current ranged ±2 nA. The current onset was detected at ~ 0.05 V for this sample.

The size of the nanostructures did not show apparent differences in I-V profiles. Regarding the Coulombic profiles of Co-Por **1**, there have been previous reports of current profiles with Coulombic staircase characteristics obtained at room temperature.[39,40] Wakayama et al. reported that organic molecules could be used as Coulomb islands of single-electron tunneling devices; a porphyrin derivative (tetrakis-3,5 di-*t*-butylphenyl-porphyrin (H_2-TBPP)) was found to be suitable as a Coulomb island. The H_2-TBPP was layered between SiO_2 on Si(100) and was investigated with STM at 5K under ultra-high vacuum.[41]

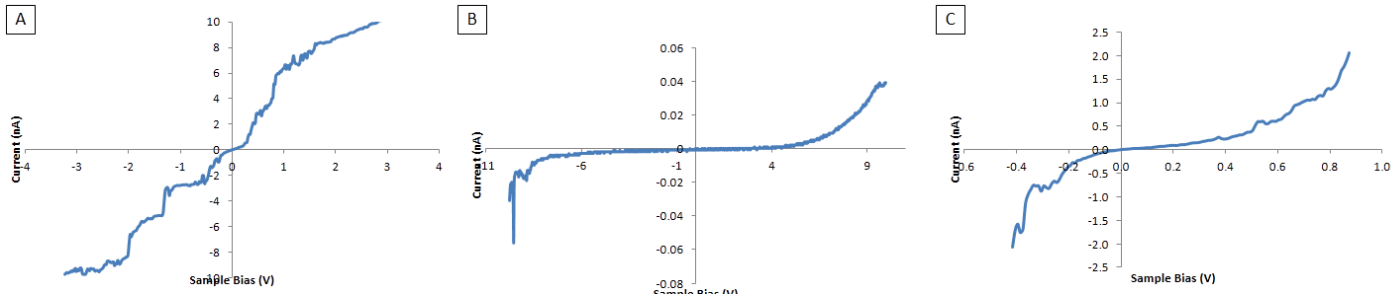

Figure 5. Height distribution measured with cursor profiles for cobaltacarborane porphyrins (n = 100): (A) Co-Por **1**; (B) Co-Por **2**; and (C) Co-Por **3**.

The selected cobaltacarborane porphyrins provide an interesting comparison of how the length of the pathways influence the transport of electrons through the molecules. The asymmetric arrangement of substituents for CoPor **1** resulted in a molecular pathway that produced a staircase shaped I-V profile. Both the molecular configuration and size of nanostructures of Co-Por **2** and CoPor **3** influenced the magnitude and symmetry of I-V profiles (Figure 5). Comparing **2** and **3** we observe that the larger (Co-Por **2**) nanostructures sustained a wider range of current, whereas the smaller nanoislands of Co-Por **3** ranged within ±1 V.

4. Conclusion

In the future, the conductive properties of selected molecular architectures will be accurately computed using theoretical approaches. However, currently there is a need for accurate and reproducible experimental measurements of conductive properties of molecular architectures for

reliable comparison to theoretical models of charge transport in molecular systems. Systematic changes in surface shapes and dispersity shown with AFM images of porphyrin nanostructures illustrated the critical role of molecular structure for the self-assembly of cobaltacarborane porphyrins on surfaces. The conductive properties of cobaltacarborane porphyrins changed according to the numbers and arrangement of substituents. It is critical to know the organization and arrangement of molecules on surfaces when modeling charge transport. We anticipate that well-defined arrangements of molecules and aggregates on surfaces will lead to accurate and reproducible local measurements of charge transport for different pathways through the molecules and provide insight on structure/property relationships.

Acknowledgments

The authors gratefully acknowledge support from the National Science Foundation (DMR-0906873), the National Institutes of Health (R01 CA179902), the American Chemical Society Petroleum Research Fund (New Directions Program) and the Camille Dreyfus Teacher-Scholar Program. The authors also thank L. E. Englade-Franklin for careful editing and manuscript review.

Conflict of Interest

The authors declare no competing financial interest.

References

1. Fox MA (1999) Fundamentals in the Design of Molecular Electronic Devices: Long- Range Charge Carrier Transport and Electronic Coupling. *Acc Chem Res* 32: 201–207.
2. Liu C-Y, Pan H-L, Fox MA, et al. (1993) High-Density Nanosecond Charge Trapping in Thin-Films of the Photoconductor ZnODEP. *Science* 261: 897–899.
3. Adams DM, Kerimo J, Liu C-Y, et al. (2000) Electric field modulated near-field photo-luminescence of organic thin films. *J Phys Chem B* 104: 6728–6736.
4. Kimura M, Saito Y, Ohta K, et al. (2002) Self-Organization of Supramolecular Complex Composed of Rigid Dendritic Porphyrin and Fullerene. *J Am Chem Soc* 124: 5274–5275.
5. Burrows HD, Gonsalves AMR, Leitao MLP, et al. (1997) Phase transitions and self-assembly in meso-tetrakis(undecyl)porphyrin. *Supramolec Sci* 4: 241–246.
6. Tsuda A, Osuka A (2001) Fully Conjugated Porphyrin Tapes with Electronic Absorption Bands That Reach into Infrared. *Science* 293: 79–82.
7. Reimers JR, Hall LE, Crossley MJ, et al. (1999) Rigid fused Oligoporphyrins as Potential Versatile Molecular Wires. 2. B3LYP and SCF Calculated Geometric and Electronic Properties of 98 Oligoporphyrin and Related Molecules. *J Phys Chem A* 103: 4385–4397.
8. Jiao J, Anariba F, Tiznado H, et al. (2006) Stepwise Formation and Characterization of Covalently Linked Multiporphyrin-Imid Architectures on Si(100). *J Am Chem Soc* 128: 6965–6974.
9. Roth KM, Liu Z, Gryko DT, et al. (2003) Charge-Retention Characteristics of Self-Assembled Monolayers of Molecular-Wire-Linked Porphyrins on Gold (Chapter 5). In: Lieberman M, editor. *Molecules as Components of Electronic Devices*. Washington DC: Oxford University Press.

10. Liu C-Y, Pan HL, Fox MA, et al. (1997) Reversible charge trapping/detrapping in a photoconductive insulator of liquid crystal zinc porphyrin. *Chem Mater* 9: 1422–1429.
11. Roth KM, Dontha N, Dabke RB, et al. (2000) Molecular approach toward information storage based on the redox properties of porphyrins in self-assembled monolayers. *J Vac Sci Technol* 18: 2359–2364.
12. Malinski T, Taha Z (1992) Nitric-Oxide Release from a Single Cell Measured In Situ by a Porphyrinic-Based Microsensor. *Nature* 358: 676–678.
13. Filippini D, Alimelli A, Natale CD, et al. (1999) Chemical Sensing with Familiar Devices. *Angew Chem Int Ed* 45: 3800–3803.
14. Maree CHM, Roosendaal SJ, Savenije TJ, et al. (1996) Photovoltaic effects in porphyrin polymer films and heterojunctions. *J Appl Phys* 80: 3381–3389.
15. Murata K, Ito S, Takahashi K, et al. (1997) Photocurrent from photocorrosion of aluminum electrode in porphyrin/Al Schottky-barrier cells. *Appl Phys Lett* 71: 674–676.
16. Harima Y, Okazaki H, Kunugi Y, et al. (1996) Formation of Schottky barriers at interfaces between metals and molecular semiconductors of p- and n-type conductances. *Appl Phys Lett* 69: 1059–1061.
17. Chowdhury A, Chowdhury J, Pal P, et al. (1998) Light-emitting diodes from molecularly thin porphyrin derivative: Effect of molecular packing. *Solid State Commun* 107: 725–729.
18. Baldo MA, O'Brien DF, You Y, et al. (1998) Highly efficient phosphorescent emission from organic electroluminescent devices. *Nature* 395: 151–154.
19. Kwong RC, Sibley S, Dubovoy T, et al. (1999) Efficient, saturated red organic light emitting devices based on phosphorescent platinum(II) porphyrins. *Chem Mater* 11: 3709–3713.
20. Sendt K, Johnston LA, Hough WA, et al. (2002) Switchable Electronic Coupling in Model Oligoporphyrin Molecular Wires Examined through the Measurement and Assignment of Electronic Absorption Spectra. *J Am Chem Soc* 124: 9299–9309.
21. Reimers JR, Lu TX, Crossley MJ, et al. (1996) Molecular electronic properties of fused rigid porphyrin-oligomer molecular wires. *Chem Phys Lett* 256: 353–359.
22. Robertson N, McGowan CA (2003) A comparison of potential molecular wires as components for molecular electronics. *Chem Soc Rev* 32: 96–103.
23. Hao E, Jensen TJ, Courtney BH, et al. (2005) Synthesis and cellular studies of porphyrin−cobaltacarborane conjugates. *Bioconjugate Chem* 16: 1495–1502.
24. Hao E, Sibrian-Vazquez M, Serem W, et al. (2007) Synthesis, aggregation and cellular investigations of porphyrin–cobaltacarborane conjugates. *Chem A Eur J* 13: 9035–9042.
25. Hao E, Zhang M, E W, et al. (2008) Synthesis and spectroelectrochemistry of N-cobaltacarborane porphyrin conjugates. *Bioconjugate Chem* 19: 2171–2181.
26. Hao E, Vicente MGH (2005) Expeditious synthesis of porphyrin-cobaltacarborane conjugates. *Chem Commun* 1306–1308.
27. Sibrian-Vazquez M, Hao E, Jensen TJ, et al. (2006) Enhanced cellular uptake with a cobaltacarborane−porphyrin−HIV-1 Tat 48−60 conjugate. *Bioconjugate Chemistry* 17: 928–934.
28. Friedbacher G, Fuchs H (1999) Classification of scanning probe microscopies - (Technical report). *Pure Appl Chem* 71: 1337–1357.
29. Ogunrinde A, Hipps KW, Scudiero L (2006) A scanning tunneling microscopy study of self-assembled nickel(II) octaethylporphyrin deposited from solutions on HOPG. *Langmuir* 22: 5697–5701.

30. Palermo V, Palma M, Samori P (2006) Electronic characterization of organic thin films by Kelvin probe force microscopy. *Adv Mater* 18: 145–164.
31. Kronik L, Shapira Y (1999) Surface photovoltage phenomena: theory, experiment, and applications. *Surf Sci Rep* 37: 1–206.
32. Matey JR, Blanc J (1985) Scanning capacitance microscopy. *J Appl Phys* 57: 1437–1444.
33. Xu S, Arnsdorf MF (1995) Electrostatic force microscope for probing surface charges in aqueous solutions. *Proc Natl Acad Sci* 92: 10384–10388.
34. Afsharimani N, Nysten B (2013) Scanning probe microscopy study of electronic properties in alkyl-substituted oligothiophene-based field-effect transitors. *Vacuum* 90: 17–24.
35. Jean MS, Hudlet S, Guthmann C, et al. (1999) Van der Waals and capacitive forces in atomic force microscopies. *J Appl Phys* 86: 5245–5248.
36. Kodera M, Yoshimizu Y, Uchida K (2012) Potential Characterization of Interconnect Corrosion by Kelvin Probe and Electrostatic Force Microscopies. *Japan J Appl Phys* 51.
37. Necas D, Klapetek P (2012) Gwyddion: an open-source software for SPM data analysis. *Cent Eur J Phys* 10: 181–188.
38. Hao E (2007) Syntheseses and evaluation of porphyrin derivatives for applications in medicine and in material science. Baton Rouge, LA: Dissertation, Louisiana State University.
39. Matsumoto K, Ishii M, Segawa K, et al. (1996) Room temperature operation of a single electron transistor made by the scanning tunneling microscope nanooxidation process for the TiO_x/Ti system. *Appl Phys Lett* 68: 34–36.
40. Kim TW, Choo DC, Shim JH, et al. (2001) Nanocrystals acting as Coulomb islands operating at room temperature created using a focused ion-beam process. *Appl Phys Lett* 79: 120–122.
41. Wakayama Y, Kubota T, Suzuki H, et al. (2003) Molecular Coulomb islands for single-electron tunneling in SiO_2/molecular layer/SiO_2 multilayers on Si(100). *J Appl Phys* 94: 4711–4713.

AIMS Press